EFFECT OF FLUCTUATING SURFACE STRUCTURE AND FREE ENERGY ON THE GROWTH OF LINEAR TUBULAR AGGREGATES

TERRELL L. HILL
Laboratory of Molecular Biology, National Institute of Arthritis, Diabetes, and Digestive and Kidney Diseases, National Institutes of Health, Bethesda, Maryland 20205

ABSTRACT Simple linear tubular aggregates with up to eight strands are studied theoretically at equilibrium and under conditions of steady growth or shortening. The surface structure and free energy at an end of the polymer fluctuate as a consequence of the gain or loss of individual subunits. The surface free energy governs the probability distribution of surface structures at equilibrium. At steady state, on and off rate constants are crucial for this purpose; these depend on the gain or loss of neighbor interactions at the polymer end when a subunit is gained or lost. The observed on and off rate constants are averages of microscopic rate constants. A consequence of this is that the subunit flux onto the polymer end is, in general, not a linear function of the free subunit concentration, as is usually assumed. Monte Carlo calculations are needed at steady state for three or more strands. The general approach can be applied to microtubules, which have 13 strands. Actin is a special case, included here, with two strands.

INTRODUCTION

This paper provides an introductory treatment of the surface free energy, which is related to molecular roughness, at an end of a tubular linear polymer or aggregate comprised of s strands. Structural roughness arises as a consequence of gain or loss of individual subunits from the polymer end; the polymer is in a solution of free subunits at concentration c. The polymer end may be in a dynamic equilibrium with the free subunits ($c = c_e$) or may be gaining or losing subunits at a steady rate ($c \neq c_e$).

The inspiration for this study is the aggregation of microtubules, which have 13 strands ($s = 13$). However, much simpler cases are examined here, as a preliminary to a consideration of the microtubule problem. These simpler cases have their own intrinsic interest because surface roughness would be a general property of multistranded aggregates. Also, these cases demonstrate that the usual linear subunit flux equation, $J = \alpha c - \beta$ (J is the mean rate of addition of subunits to a polymer end, α is the second-order on rate constant, and β is the first-order off rate constant), would not generally be expected for multistranded polymers ($s > 1$); i.e., $J(c)$ is nonlinear. This point was made briefly in an earlier paper (1).

This work is concerned exclusively with so-called "equilibrium polymers," not "steady-state polymers" (1). In the latter class, a chemical reaction accompanies subunit aggregation or follows it after a lag (e.g., GTP hydrolysis occurs in microtubules and ATP hydrolysis in actin). In the former class, the one we consider, subunit addition or loss is a purely physical process (this would be the case with microtubules and actin, as well, if for example, nonhydrolyzable analogues of GTP or ATP were used). Delayed NTPase activity in steady-state polymers, mentioned above, is itself a source of strong nonlinear $J(c)$ behavior (2).

1. GENERAL DISCUSSION OF THE MODELS

In this paper we consider simple tubular aggregates constructed from hypothetical isotropic subunits or blocks (e.g., protein molecules) that are generally staggered helically (Fig. 1 *a*) but may be aligned horizontally as a limiting case (Fig. 1 *c*). Fig 1 *b* is a transverse section showing, for $s = 3$, that $i = 3$ is a neighbor of $i = 1$ (to form a tube). Fig. 1 *a* is the case $s = 3$ in which the principal neighbor to the right of any subunit is raised $\frac{1}{3}$ of a subunit height, thus forming a one-start right-handed helix (which we designate 1:3). Viewed as a left-handed helix, this same structure would be designated 2:3. Hence the right-handed cases 1:3 and 2:3 would have the same kinetic and thermodynamic properties; we need not consider both cases. The same is true for any pair s':s and s–s':s (e.g., 5:13 and 8:13 in a microtubule).

We shall assume in all models that there are no lattice vacancies (each strand is solid to its end), that subunits do not migrate from one strand to another (i.e., surface structures, as in Figs. 1 *a* and 1 *c*, change only by subunit on and off transitions), and that vibrational partition functions of subunits do not contribute significantly to the surface free energy differences introduced below, and hence can be ignored.

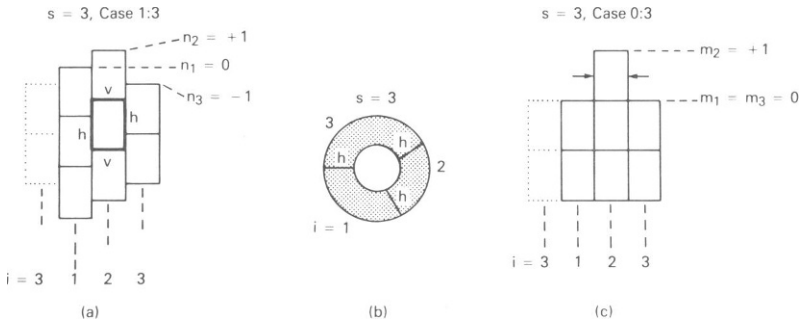

FIGURE 1 (*a*) Tip of three stranded ($i = 1, 2, 3$) "staggered" tubular polymer with ⅓ vertical rise as i increases. Dotted subunits ($i = 3$) show tubular structure. Vertical neighbor interaction v; horizontal interaction h. Height of a strand (n_i) is measured in thirds of a subunit height, relative to $n_1 = 0$. (*b*) Cross-sectional view of three-stranded tubular polymer. (*c*) "Aligned" tubular polymer with three strands. The m_i measure strand height in full subunit heights, relative to $m_1 = 0$. Arrows indicate missing horizontal interactions.

For any case s':s, in the bulk polymer (tube) each subunit (e.g., see the heavy subunit in Fig. 1 *a*) interacts with both horizontal (h) and vertical (v) nearest neighbors. Let w_h and w_v be full subunit-subunit nearest-neighbor interaction free energies (these are negative quantities relative to a zero at infinite separation). Any given bulk subunit (e.g., the heavy subunit in Fig. 1 *a*) is involved in interactions with total free energy $2w_v + 2w_h$, but only half of this can be assigned to the given subunit. Thus, bulk polymer with N subunits has a total interaction free energy $N(w_v + w_h)$.

If a long polymer with $2N$ is broken in half to form two new ends and surfaces, s vertical interactions and $2m$ horizontal interactions are lost, where $m \geq 0$ depends on the surface structures created in the break; m may be a fraction. After the break, the total polymer interaction free energy is

$$2N(w_v + w_h) - sw_v - 2mw_h.$$

This is larger (w_v and w_h are negative) than the pre-break free energy $2N(w_v + w_h)$. The difference in the two quantities, per end, is the surface free energy of one (either) end

$$G_s = -(s/2)w_v - mw_h. \quad (1)$$

This is a positive quantity. The vertical contribution to G_s, $-sw_v/2$, is the same for every break, but the horizontal contribution depends on m. Thus the term $-mw_h$ is the interesting part of G_s; m is an index of molecular roughness at the polymer end.

For example, if the surface structure in Fig. 1 *c* is thought of as having been formed by a break, two horizontal interactions are missing (arrows): $2m = 2$ and $m = 1$. Incidentally, the minimum possible value of m for this polymer is $m = 0$. In Fig. 1 *a*, missing horizontal interactions at the surface are ⅓ (between strands $i = 1, 2$), ⅔ ($i = 2, 3$), and ⅓ ($i = 3, 1$). Thus, $2m = 4/3$ and $m = 2/3$. This is actually the minimum possible value of m for this case (1:3).

For any given surface structure, m may be calculated systematically as follows. In the special (aligned) case 0:s (as in Fig. 1 *c*), we arbitrarily select strand $i = 1$ as the reference strand and assign the position of its end the value $m_1 \equiv 0$. The position (height) of the end or tip of each strand $i = 2, \ldots, s$ is then measured relative to the end of strand $i = 1$, in units of subunit height, and denoted m_i, which may be a positive or negative integer, or zero. For example, in Fig. 1 *c*, $m_2 = 1$ and $m_3 = 0$. Then

$$m = (|m_2| + |m_3 - m_2| + |m_4 - m_3| + \cdots + |m_s - m_{s-1}| + |m_s|)/2. \quad (2)$$

The sum here is a measure of the amount of exposed vertical surface at the polymer end and hence a measure of missing horizontal interactions and of molecular roughness.

In other cases s':s, with $s' > 0$ (staggered), for convenience we first measure the amount of vertical surface not in integral units (as above) but in fractional units $1/s$. Just as m_i measures the height of the end of strand i relative to the end of strand 1 in units of subunit height, here we use n_i to express the same quantity in units of $1/s$ of the subunit height. As before, $n_1 \equiv 0$. The n_i are positive or negative integers, or zero. Hence

$$m = (|n_2| + |n_3 - n_2| + \cdots + |n_s - n_{s-1}| + |n_s|)/2s. \quad (3)$$

The division by s here corrects for the fractional units ($1/s$) used. That is, $|n_2| = s|m_2|$, etc. As an example, in Fig. 1 *a*, the sum in Eq. 3 is $1 + 2 + 1 = 4$ and $m = 4/6 = 2/3$ (as already found).

Equilibrium Surface Partition Function

When the polymer end is in equilibrium with free subunits ($c = c_e$) via on and off transitions, the polymer end will pass, stochastically, through (in principle) an infinite number of discrete surface structures, each with a definite value of m, as calculated from Eq. 2 or Eq. 3. There is a Boltzmann probability distribution at equilibrium among these structures, a structure with m having a relative weight $e^{mw_h/kT} = x^m$, where $0 \leq x \equiv e^{w_h/kT} \leq 1$. The limiting

case $x = 1$ (i.e., $w_h = 0$) corresponds to independent strands. Also, when $w_h \to -\infty$, $x \to 0$. The larger the value of m, the rougher the surface, the larger the surface free energy (Eq. 1), and the lower the relative weight of the state. Note that w_v is not involved here because the w_v term in Eq. 1 is the same for all structures.

In staggered cases, to avoid fractions, it is usually convenient (but not necessary) to introduce $n = sm$ and $y = x^{1/s}$ so that $x^m = x^{n/s} = y^n$. In realistic cases both x and y lie between 0 and 1.

All possible surface structures can be generated by allowing each of m_2 to m_s in Eq. 2 (aligned cases) or each of n_2 to n_s in Eq. 3 (staggered cases) to take on all possible values from $-\infty$ to $+\infty$. Several or many structures so generated may have the same value of m. Let $R(m)$ be the number of structures (degeneracy) with a particular m. Then the surface partition function, the sum over all surface states, is

$$Q = \sum_m R(m)x^m = \sum_n S(n)\,y^n, \tag{4}$$

where these sums are over all possible values of $m \geq 0$ or $n \geq 0$ and $R(m) = S(n)$ is the degeneracy. In nontrivial cases, early $R(m)$ or $S(n)$ can be found by computer enumeration. In many cases Q can be expressed in closed form (see Sections 2 and 4).

It should be noticed that we are not concerned here with the length of the polymer, which has large fluctuations (1), but only with the distribution in surface structures (at the polymer end), which have different values of m corresponding to different degrees of molecular roughness.

The probability that the surface has a particular value of m or n is

$$P_m = R(m)x^m/Q = P_n^* = S(n)y^n/Q. \tag{5}$$

The asterisk is used when the index is $n = sm$. From this it follows that

$$\overline{m} = \frac{x}{Q}\frac{dQ}{dx} = \frac{1}{s}\frac{y}{Q}\frac{dQ}{dy} \tag{6}$$

$$\sigma_m^2 = x\frac{d\overline{m}}{dx} = \frac{1}{s}y\frac{d\overline{m}}{dy}, \tag{7}$$

where $\overline{m}$ is the mean value of m and σ_m^2 is the variance in m.

Because all strands are equivalent (at equilibrium or steady state), the mean values of the separate terms in the sums in Eqs. 2 and 3 must all be equal. Hence

$$\overline{m} = s\overline{q}/2 = \overline{r}/2, \tag{8}$$

where q and r are used here to represent any one of the terms in the sum in Eq. 2 or 3, respectively, for example, $|m_2|$ or $|n_2|$. Of course $r = sq$.

Although it is easy to calculate the mean values $\overline{q}$ or $\overline{r}$ (from $\overline{m}$, Eq. 8), the complete probability distribution in q or r requires further details, which we turn to below. This distribution is of some interest because P_m or P_n^* gives the distribution in molecular roughness for the complete surface but the probability distribution in q or r refers to the individual elements of roughness (height difference) between two neighboring strands.

Each of the $R(m)$ surface structures with the same m value has the same weight in the equilibrium distribution. Also, each of these structures has s values of q (Eq. 2), all with the same weight. Some of these q values may be repeats. The total number of q values for a given m is then $sR(m)$. Of these, let $W(q, m)$ be the number with a particular value of q. Then $\Sigma_q W(q, m) = sR(m)$. The probability of a given m and also a given q is then

$$\frac{R(m)x^m}{Q} \cdot \frac{W(q, m)}{sR(m)} = \frac{W(q, m)x^m}{sQ}. \tag{9}$$

Then the probability of a given q, irrespective of the m value, is

$$p_q = \frac{1}{sQ}\sum_m W(q, m)x^m. \tag{10}$$

This is the desired probability distribution in q (e.g., $|m_2|$). Values of $W(q, m)$, for q and m not too large, can be found by computer enumeration. Closed expressions for the p_q can be obtained in some cases (see Sections 2 and 4). With the p_q available, at least in principle one can calculate, for example, the mean $\overline{q}$ (already known from $\overline{m}$, Eq. 8) and the variance σ_q^2. Note that the series in Eq. 10 has x to the power m, not q. Hence equations like Eqs. 6 and 7 are not applicable.

Exactly the same argument applies if we use (for staggered cases) the n_i and r (Eq. 3) in place of the m_i and q (Eq. 2). The result is

$$p_r^*(= p_q) = \frac{1}{sQ}\sum_n U(r, n)y^n, \tag{11}$$

where the asterisk is used for the index $r = sq$, and $U(r, n)$ $(= W(q, m))$ is the number of occurrences of a particular value of r among the $sS(n)$ terms in Eq. 3 for the $S(n)$ surface structures with a given value of n. Just as $\overline{r} = s\overline{q}$, we also have $\sigma_r^2 = s^2\sigma_q^2$. The two modes of calculation (m_i, q; n_i, r) are completely equivalent; the choice is a matter of notational convenience only.

Rate Constants and Detailed Balance

Consider, at equilibrium, a particular surface structure or state λ and another structure or state ν that is reached from λ on the addition of one subunit from solution ($c = c_e$) onto the end of one of the s strands of the polymer originally in state λ. Aside from the change in surface structure, in effect one subunit has been added to the bulk polymer. However, this does not involve any free energy change because of the equilibrium between polymer and solution. The values of m in the two states are designated $m(\lambda)$ and

$m(\nu)$. The change in surface free energy in the process $\lambda \rightarrow \nu$ is then (Eq. 1)

$$\Delta G_s = [-m(\nu)w_h] - [-m(\lambda)w_h] = [m(\lambda) - m(\nu)]w_h. \quad (12)$$

The ratio of the probabilities of the two states (at equilibrium) is

$$\mathbf{p}_\nu^e/\mathbf{p}_\lambda^e = e^{-\Delta G_s/kT} = e^{m(\nu)w_h/kT}/e^{m(\lambda)w_h/kT}. \quad (13)$$

Let $\alpha_{\lambda\nu}$ be the second-order rate constant for the on process, $\lambda \rightarrow \nu$, and let $\beta_{\nu\lambda}$ be the first-order off rate constant for $\nu \rightarrow \lambda$. Because of detailed balance between the two states at equilibrium,

$$\alpha_{\lambda\nu}c_e\mathbf{p}_\lambda^e = \beta_{\nu\lambda}\mathbf{p}_\nu^e. \quad (14)$$

Reference on and off rate constants, α and β, are defined and apply when $\Delta G_s = 0$. Examples with $\Delta G_s = 0$ are shown in Fig. 2. The constants $\alpha_{\lambda\nu}$ and $\beta_{\nu\lambda}$ differ from α and β, respectively, because of the surface free energy change. When states λ and ν are such that $\Delta G_s = 0$,

$$\alpha c_e\mathbf{p}_\lambda^e = \beta\mathbf{p}_\nu^e, \quad \mathbf{p}_\nu^e = \mathbf{p}_\lambda^e, \quad \text{and } \alpha c_e = \beta. \quad (15)$$

In the general case ($\Delta G_s \neq 0$), then,

$$\frac{\mathbf{p}_\nu^e}{\mathbf{p}_\lambda^e} = e^{-\Delta G_s/kT} = \frac{\alpha_{\lambda\nu}\,c_e}{\beta_{\nu\lambda}} = \frac{\alpha_{\lambda\nu}/\alpha}{\beta_{\nu\lambda}/\beta}. \quad (16)$$

If we put $\alpha_{\lambda\nu} = \alpha a_{\lambda\nu}$ and $\beta_{\nu\lambda} = \beta b_{\nu\lambda}$, then $a_{\lambda\nu}$ and $b_{\nu\lambda}$ are factors that perturb the reference rate constants that arise from the surface free energy change ΔG_s in the process $\lambda \rightarrow \nu$. The factor $e^{-\Delta G_s/kT}$ is the corresponding perturbation of the equilibrium ratio $\mathbf{p}_\nu^e/\mathbf{p}_\lambda^e$ (which is equal to 1 if $\Delta G_s = 0$); $e^{-\Delta G_s/kT}$ is split between the rate constant perturbation factors $a_{\lambda\nu}$ and $b_{\nu\lambda}$ in such a way that $e^{-\Delta G_s/kT} = a_{\lambda\nu}/b_{\nu\lambda}$ (Eq. 16). A practical way to express this will be introduced in Section 3.

At equilibrium ($c = c_e$) or steady state (i.e., steady growth or steady shortening of the polymer when $c \neq c_e$), the subunit on rate for the particular process $\lambda \rightarrow \nu$ is $\alpha_{\lambda\nu}c\mathbf{p}_\lambda$ (Eq. 14). The $\mathbf{p}_\lambda$ are state probabilities at steady state. The total on rate for state λ is then $\Sigma_\nu\alpha_{\lambda\nu}c\mathbf{p}_\lambda$, where the sum is over the s possible values of ν (i.e., a subunit may be added to the end of any one of the s strands in state λ). If we now sum over all individual surface states λ, we obtain the mean subunit on rate for the s-stranded polymer

$$c\sum_{\nu,\lambda}\alpha_{\lambda\nu}\mathbf{p}_\lambda = \bar{\alpha}cs, \quad \bar{\alpha} = (1/s)\sum_{\nu,\lambda}\alpha_{\lambda\nu}\mathbf{p}_\lambda, \quad (17)$$

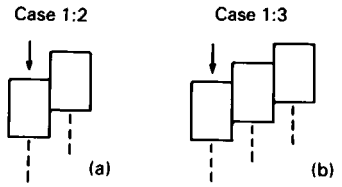

FIGURE 2 Two examples in which addition of a subunit (arrow) does not change surface free energy.

where $\bar{\alpha}$ is the mean (operational) on rate constant per strand. Similarly, on summing the subunit off rate $\beta_{\nu\lambda}\mathbf{p}_\nu$ over ν and λ, we obtain $\bar{\beta}$, the mean off rate constant per strand

$$\sum_{\nu,\lambda}\beta_{\nu\lambda}\mathbf{p}_\nu = \bar{\beta}s, \quad \bar{\beta} = (1/s)\sum_{\nu,\lambda}\beta_{\nu\lambda}\mathbf{p}_\nu. \quad (18)$$

The mean subunit flux per strand is then $J(c) = \bar{\alpha}c - \bar{\beta}$. We shall find in Sections 3 and 5 that, in general, $\bar{\alpha}$ and $\bar{\beta}$ depend on c, and hence that $J(c)$ is nonlinear. Except in very simple cases the steady-state probabilities $\mathbf{p}_\lambda$, needed above, cannot be found analytically. Instead we use (Sections 3 and 5) Monte Carlo simulation to obtain $J(c)$ and other properties of the polymer end.

If, at equilibrium, we sum both sides of the detailed-balance Eq. 14 over ν and λ we obtain

$$c_e\sum_{\nu,\lambda}\alpha_{\lambda\nu}\mathbf{p}_\lambda^e = \bar{\alpha}_e c_e s = \sum_{\nu,\lambda}\beta_{\nu\lambda}\mathbf{p}_\nu^e = \bar{\beta}_e s. \quad (19)$$

Thus (Eq. 15),

$$c_e = \beta/\alpha = \bar{\beta}_e/\bar{\alpha}_e. \quad (20)$$

Incidentally, if tip subunits moved from strand to strand rapidly compared to on and off transitions (we are assuming the opposite in this paper), the equilibrium distribution $\mathbf{p}_\lambda^e$ among the surface states would be maintained even when $c \neq c_e$. In this hypothetical case, $J = \bar{\alpha}_e c - \bar{\beta}_e$ and $J(c)$ would be linear (1). However, in general, the steady-state $\mathbf{p}_\lambda$ depend on c and hence $\bar{\alpha}$ and $\bar{\beta}$ depend on c.

The remainder of the paper is devoted to a number of special cases, including some numerical results.

2. EQUILIBRIUM PROPERTIES OF ALIGNED MODELS

In this section we consider, at equilibrium, cases of the type 0:s, as illustrated in Fig. 1 *c*. For $s = 2$ (also regarded as a tube, as in Fig. 3 *a*), one strand always ends at $m_1 = 0$ and the other ends at $m_2 = 0, \pm 1, \pm 2, \ldots$ (Fig. 3 *b*). The value of m (Eq. 2) is simply $|m_2|$; that is, m is the height difference between the two strands, measured in subunit heights.

The horizontal interaction free energy between two

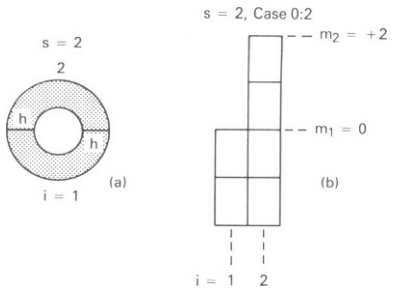

FIGURE 3 Two-stranded tubular aligned model showing (*a*) cross-sectional view and (*b*) a tip structure.

subunits is $2w_h$ (Fig. 3 *a*). This assignment is made to include $s = 2$ in the sequence of tubes $s = 3, 4, \ldots$. For a model with two piles of aligned cubic blocks (not a tube), the properties are the same as derived below if the horizontal interaction free energy between two blocks is called $2w_h$.

All possible surface structures or states are enumerated by m_2. The state with $m = m_2 = 0$ (flat surface) is the most stable and has a term 1 in Q (Eq. 4). The next most stable states are $m_2 = \pm 1$, each with a term $x = e^{w_h/kT}$ in Q, etc. The complete Q is

$$Q = 1 + 2(x + x^2 + x^3 + \cdots) = (1 + x)/(1 - x). \quad (21)$$

Probabilities of the various m values are (Eq. 5)

$$P_0 = 1/Q, \quad P_m = 2x^m/Q \quad (m \geq 1). \quad (22)$$

From Eqs. 6 and 7, the mean and variance are

$$\overline{m} = 2x/(1 - x^2), \quad \sigma_m^2 = 2x(1 + x^2)/(1 - x^2)^2. \quad (23)$$

The bottom curve in Fig. 4 shows $\overline{m}$ for this case as a function of $-w_h/kT$. Strong horizontal attractions in the polymer ($x \to 0$) cause $P_0 \to 1$ and $\overline{m} \to 0$ (flat surface); weak horizontal attractions ($x \to 1$, independent strands) lead to $\overline{m} \to \infty$. Vertical interactions (w_v) are not involved in surface roughness.

For $s = 3$ (Fig 1 *c*), for $m_1 \equiv 0$ and each of $m_2 = 0, \pm 1, \pm 2, \ldots$, one can sum x^m from $m_3 = -\infty$ to $+\infty$. These series are then summed (over m_2) to obtain

$$Q = (1 + 4x + x^2)/(1 - x)^2. \quad (24)$$

An alternative procedure for finding Q, practical for $s = 3, 4, 5$ but not beyond, is to express Q as the trace of a matrix product. This is possible because this is a type of linear nearest-neighbor interaction problem (3). I am indebted to Dr. T. Tsuchiya for confirming Q in this way for $s = 3, 4, 5$. The most practical method, however, up to about $s = 8$, is to enumerate individual surface states by computer, letting $m_2, m_3, \ldots$ range as far as necessary on either side of zero. The value of m is calculated (in the computer program) for each state (Eq. 2) and tallied, to provide the $R(m)$ values in Eq. 4. If $R(m)$ extends accurately to large enough m, Newton's forward interpolation formula applied to successive $R(m)$ values can be used to find $R(m)$ as a polynomial in m. Summation over m (Eq. 4) then gives a closed expression for Q. The $s = 3$ case is especially simple (Newton's formula is not needed):

$$Q = 1 + 6x + 12x^2 + 18x^3 + 24x^4 + \cdots$$
$$= 1 + [6x/(1 - x)^2], \quad (25)$$

which again leads to Eq. 24.

Probabilities of different m values for $s = 3$ are (Eqs. 5 and 25)

$$P_0 = 1/Q, \quad P_m = 6mx^m/Q \quad (m \geq 1). \quad (26)$$

From Eqs. 6 and 7,

$$\overline{m} = \frac{6x(1 + x)}{(1 - x)(1 + 4x + x^2)} \quad (27)$$

$$\sigma_m^2 = \frac{6x(1 + 2x + 6x^2 + 2x^3 + x^4)}{(1 - x)^2(1 + 4x + x^2)^2}. \quad (28)$$

The curve $\overline{m}(-w_h/kT)$ is included in Fig. 4.

The mean height difference between neighboring strands is $\overline{q} = \overline{|m_2|} = 2\overline{m}/3$ (Eq. 8). For example, at $x = 0.5$, $\overline{m} = 2.769$ (Eq. 27) and $\overline{q} = 1.846$. To find the probability distribution in q (Eq. 10), $W(q, m)$ is needed. These numbers can be obtained in the same computer program mentioned above by tallying the $3R(m)$ values of q for each m according to q value. Table I gives $W(q, m)$ for this case for small values of q and m (the pattern is obvious from this fragment but the computing went well beyond Table I). From Eq. 10, then, we obtain

$$p_0 = (1 - x^2)/(1 + 4x + x^2) \quad (29)$$

$$p_q = \frac{2[(q + 1)x^q - (q - 1)x^{q+1}](1 - x)}{(1 + 4x + x^2)} \quad (q \geq 1). \quad (30)$$

As a check, one finds $\Sigma_q p_q = 1$. Numerical values of the p_q are given in Table II for $x = 0.5$. The most likely neighbor height differences are $q = 0$, 1, and 2, but convergence in p_q is rather slow at large q.

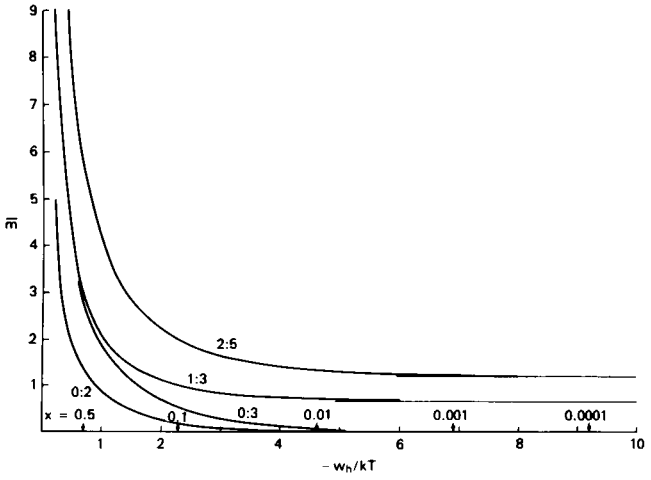

FIGURE 4 Curves of $\overline{m}$ as a function of $-w_h/kT$ ($x = e^{w_h/kT}$) for four different cases, all at equilibrium.

TABLE I
INITIAL VALUES OF $W(q,m)$ FOR THE CASE 0:3

m =	0	1	2	3	4
q = 0	3	6	6	6	6
1		12	12	12	12
2			18	12	12
3				24	12
4					30

TABLE II
VALUES OF p_q FOR THE CASE 0:3 AT $x = 0.5$

q	p_q	q	p_q
0	0.2308	6	0.0216
1	0.3077	7	0.0120
2	0.1923	8	0.0066
3	0.1154	9	0.0036
4	0.0673	10	0.0020
5	0.0385	11	0.0011

For $s = 4$, we find by the computer enumeration method described above,

$$Q = 1 + 12x + 42x^2 + 92x^3 + 162x^4 + 252x^5 + \cdots$$

$$= 1 + 2x \sum_{k=0}^{\infty} (6 + 10k + 5k^2)x^k \quad (31)$$

$$= (1 + 9x + 9x^2 + x^3)/(1 - x)^3. \quad (32)$$

Then, from Eq. 6,

$$\overline{m} = \frac{12x(1 + 3x + x^2)}{(1 - x)(1 + 9x + 9x^2 + x^3)}. \quad (33)$$

Table III contains values of $W(q, m)$ for this case, obtained by computer (see above). For each m, the total number of q values is $4R(m)$, where $R(m)$ is the coefficient of x^m in Eq. 31. The $q = 0$ row and the diagonal require separate treatment. Otherwise first differences in the rows are all 48. One finds from Eq. 10,

$$p_0 = (1 + 4x + x^2)(1 - x)/(1 + 9x + 9x^2 + x^3) \quad (34)$$

$$p_q = \frac{x^q}{Q}\left[(q + 1)(q + 2) + \frac{6x(q + 2 - qx)}{(1 - x)^2}\right] \quad (q \geq 1). \quad (35)$$

Again, $\Sigma_q p_q = 1$ as required.

It will be noticed in Eqs. 21, 24, and 32 ($s = 2, 3, 4$) that the coefficients in the numerator of Q are the squares of binomial coefficients. The above computer enumeration method has been used to confirm this property for $s = 5$ and 6. A less complete calculation has also been made to confirm the squared binomial coefficients for $s = 7$ and 8, as far as the central binomial coefficient (symmetry would then account for the remaining coefficients). Based on the special cases $s = 2$ to 8, the general expression for arbitrary s thus appears to be

$$Q = \frac{1}{(1 - x)^{s-1}} \sum_{k=0}^{s-1} \left[\frac{(s - 1)!}{k!(s - 1 - k)!}\right]^2 x^k. \quad (36)$$

From Eq. 6 we then find for arbitrary s

$$\overline{m} = (s - 1)sx\,\Sigma_2/(1 - x)\,\Sigma_1, \quad (37)$$

where Σ_1 is the sum in Eq. 36 and

$$\Sigma_2 = \sum_{k=0}^{s-2} \frac{(s - 1)!(s - 2)!x^k}{k!\,(s - 1 - k)!(k + 1)!(s - 2 - k)!}. \quad (38)$$

The first few Σ_2 are

$$s = 2, \Sigma_2 = 1; s = 3, \Sigma_2 = 1 + x$$

$$s = 4, \Sigma_2 = 1 + 3x + x^2$$

$$s = 5, \Sigma_2 = 1 + 6x + 6x^2 + x^3$$

$$s = 6, \Sigma_2 = 1 + 10x + 20x^2 + 10x^3 + x^4. \quad (39)$$

The sum of the coefficients in Σ_2 are the Catalan numbers 1, 2, 5, 14, 42, ...

The limit $s \to \infty$ is of theoretical interest. This refers to an infinitely wide tube with local fluctuations in roughness along the one-dimensional surface of s subunits. To study this case, we can use the familiar maximum term method in statistical mechanics (4). Let the summand in Σ_1 (Eq. 36) be denoted t_k. Then $\partial \ln t_k/\partial k = 0$, using $s \to \infty$, leads to

$$k^* = sx^{1/2}/(1 + x^{1/2}) \quad (40)$$

as that value of k which maximizes t_k. Using only this t_k in $\ln Q$, we obtain (Eq. 6)

$$\overline{m} = \frac{sx}{1 - x} + \frac{sx^{1/2}}{1 + x^{1/2}} = \frac{sx^{1/2}}{1 - x} \quad (s \to \infty), \quad (41)$$

where the term $sx/(1 - x)$ arises from the factor $(1 - x)^{s-1}$ in Q. Note that $\overline{m}$ is an extensive thermodynamic property (proportional to s). The mean nearest neighbor height difference along the surface is

$$\overline{q} = 2\overline{m}/s = 2x^{1/2}/(1 - x) \quad (s \to \infty). \quad (42)$$

At $x = 0.5$, $\overline{q} = 2.828$. For the same x, $\overline{q} = 1.333$ for $s = 2$, 1.846 for $s = 3$, and 2.095 for $s = 4$.

The variance in m is

$$\sigma_m^2 = x\frac{d\overline{m}}{dx} = \frac{sx^{1/2}(1 + x)}{2(1 - x)^2} \quad (s \to \infty). \quad (43)$$

Thus $\sigma_m^2/\overline{m}^2$ is of order $1/s \to 0$, which is normal for a fluctuating extensive thermodynamic property. The probability distribution in m is very sharp; indeed, this was

TABLE III
INITIAL VALUES OF $W(q,m)$ FOR THE CASE 0:4

$m =$	0	1	2	3	4	5
$q = 0$	4	24	48	72	96	120
1		24	72	120	168	216
2			48	96	144	192
3				80	120	168
4					120	144
5						168

already assumed (from the form of Eq. 36) in using the maximum term method.

3. ALIGNED MODELS AT STEADY STATE

Because aligned models are rather unrealistic (i.e., they have a simple square lattice), we consider in this section only $s = 2$ and $s = 3$. The $s = 2$ case (also designated 0:2) can be handled analytically and hence provides a convenient introduction to steady-state systems. The $s = 3$ case (i.e., 0:3) requires Monte Carlo calculations to obtain steady-state properties.

The 0:2 case is illustrated in Fig. 3. If we could add one subunit to the end of the polymer without changing G_s (i.e., $\Delta G_s = 0$), the reference on and off rate constants α and β would be applicable and the interaction free energy change would be $w_v + w_h$ (bulk polymer increases by one subunit). The equilibrium constant for this process would be $\alpha/\beta = 1/c_e$. Actually, for the 0:2 case, this process is hypothetical; it is necessary to add one subunit to each strand to obtain $\Delta G_s = 0$. The equilibrium constant is then $(\alpha/\beta)^2$ and the free energy change is $2(w_v + w_h)$. From either point of view,

$$1/c_e = \alpha/\beta \sim e^{-(w_v + w_h)/kT}. \tag{44}$$

This shows how α/β depends on w_v and w_h; we are not concerned here with other contributions.

In actual transitions ($\Delta G_s \neq 0$), there are two categories, as shown in Fig. 5. In Fig. 5 *a*, adding a subunit ($\lambda \rightarrow \nu$ in Eq. 12) increases m by 1. Thus $\Delta G_s = -w_h$ and (Eq. 16)

$$e^{w_h/kT} = x = \frac{\alpha_1/\alpha}{\beta_1/\beta}, \quad \frac{\alpha_1}{\beta_1} = \frac{\alpha}{\beta} \cdot x. \tag{45}$$

Similarly, in Fig. 5 *b*, adding a subunit decreases m by 1. Hence, $\Delta G_s = w_h$ and

$$e^{-w_h/kT} = \frac{1}{x} = \frac{\alpha_2/\alpha}{\beta_2/\beta}, \quad \frac{\alpha_2}{\beta_2} = \frac{\alpha}{\beta} \cdot \frac{1}{x}. \tag{46}$$

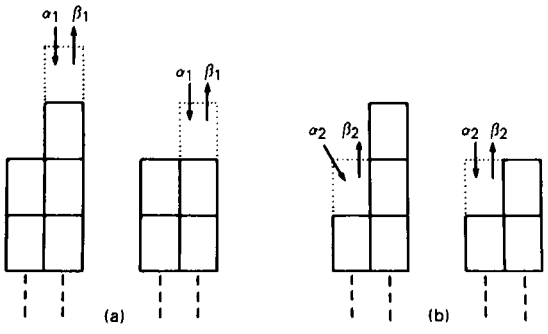

FIGURE 5 Two different pairs of rate constants, shown in (*a*) and (*b*), for the case 0:2. Dotted subunit is added, with rate constant α_1 or α_2. Removal of this subunit has rate constants β_1 and β_2.

To split $\Delta G_s \neq 0$ between α and β (see Eq. 16) in a manner consistent with Eqs. 45 and 46, we introduce the formalism (3)

$$\alpha_1 = \alpha x^{f_1}, \quad \beta_1 = \beta x^{f_1 - 1}$$
$$\alpha_2 = \alpha x^{-f_2}, \quad \beta_2 = \beta x^{1 - f_2}, \tag{47}$$

where f_1 and f_2 are constants, usually but not necessarily between 0 and 1. The factors, involving x, that modify α and β in Eqs. 47 all arise from surface free energy effects. The most realistic assumption is probably $f_1 = f_2 = 0$. That is, the on rate constant α is, say, diffusion-controlled and is not influenced by neighbor interactions (w_h). In this case, $\beta_1 = \beta x^{-1}$ and $\beta_2 = \beta x$; the full effect of ΔG_s is felt by the off rate constants (neighbor interactions must be broken for a subunit to escape).

Fig. 6 shows the kinetic diagram, at an arbitrary c, that relates the different m values. The rate constants are unchanged at larger m values. There is only one surface state at $m = 0$ (flat surface) but there are two surface states (exchange the strands) for each of $m = 1, 2, \ldots$. The steady-state probability of m is denoted P_m. Because the diagram in Fig. 6 is linear, there is a simple "detailed balance" solution for the P_m(3). One finds

$$P_0 = \frac{1 - z}{1 + z}, \quad P_m = \frac{2z^m(1 - z)}{1 + z} \quad (m \geq 1) \tag{48}$$

where

$$z(c) \equiv \frac{\alpha c x^{f_1} + \beta x^{1 - f_2}}{\beta x^{f_1 - 1} + \alpha c x^{-f_2}} = \frac{\alpha c + \beta x^{1 - f_1 - f_2}}{\beta x^{-1} + \alpha c x^{-f_1 - f_2}}. \tag{49}$$

In the special case $c = c_e = \beta/\alpha$ (equilibrium), $z = x$. Eqs. 22 and 48 are then the same. Because $P_m \sim z^m$, in analogy with Eq. 22,

$$\bar{m} = 2z/(1 - z^2), \quad \sigma_m^2 = 2z(1 + z^2)/(1 - z^2)^2, \tag{50}$$

as in Eq. 23. The average surface free energy at steady state is, from Eq. 1, $-w_v - \bar{m}w_h$, with $\bar{m}$ given by Eq. 50.

From Fig. 6, we see that the total (both strands) on rate is $2\alpha c x^{f_1}$ when $m = 0$ and is $\alpha c x^{f_1} + \alpha c x^{-f_2}$ when $m = 1, 2, \ldots$. Thus, as in Eq. 17, the mean on rate constant $\bar{\alpha}(c)$ is

$$\bar{\alpha}(c) = (1/2)[2\alpha x^{f_1} P_0 + (\alpha x^{f_1} + \alpha x^{-f_2})(P_1 + P_2 + \cdots)]$$
$$= \alpha(x^{f_1} + z x^{-f_2})/(1 + z). \tag{51}$$

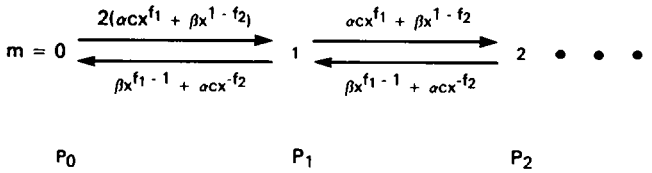

FIGURE 6 Kinetic diagram for case 0:2 in terms of m values of surface structures.

Similarly,

$$\bar{\beta}(c) = (1/2)[2\beta x^{1-f_2}P_0 + (\beta x^{f_1-1} + \beta x^{1-f_2})(P_1 + P_2 + \cdots)] = \beta(zx^{f_1-1} + x^{1-f_2})/(1+z). \quad (52)$$

Both $\bar{\alpha}$ and $\bar{\beta}$ depend on c because z is a function of c.The subunit flux per strand is $J = \bar{\alpha}c - \bar{\beta}$.

At equilibrium ($c = c_e$), $z = x$ and

$$\bar{\alpha}_e = \alpha(x^{f_1} + x^{1-f_2})/(1+x)$$
$$\bar{\beta}_e = \beta(x^{f_1} + x^{1-f_2})/(1+x). \quad (53)$$

This confirms Eq. 20 for this particular case.

In the important special case $f_1 = f_2 = 0$,

$$z = \frac{\alpha c + \beta x}{\alpha c + \beta x^{-1}}, \quad \bar{\alpha} = \alpha, \quad \bar{\beta} = \frac{\beta(z + x^2)}{x(1+z)}. \quad (54)$$

We might illustrate the involvement of Eq. 44 here. Usually, c dependence is the feature of main interest, with x assigned a fixed value. However, if the full effect of variations in w_h is to be studied, Eq. 44 cannot be ignored. In this special case ($f_1 = f_2 = 0$), it is natural to take, in Eq. 44, α as a constant and $\beta = \beta_o x$, where β_o is the value of β when $w_h = 0$ (we assume that w_v is held constant). When $w_h = 0$, the two strands are independent. Then

$$z = \frac{\alpha c + \beta_o x^2}{\alpha c + \beta_o}, \quad \bar{\alpha} = \alpha$$
$$\bar{\beta} = \frac{\beta_o[\alpha c(1 + x^2) + 2\beta_o x^2]}{2\alpha c + \beta_o(1 + x^2)}. \quad (55)$$

We shall defer numerical results until the case 1:2 in Section 5. This case (1:2) is very similar to 0:2 and is more realistic (in fact, polymerized actin is an example).

We turn now to $s = 3$, that is, case 0:3 (Fig. 1 *c*) at steady state. There are three categories of rate constants in this case, as illustrated in Fig. 7. In the solid part of the figure, $m_2 = -2$, $m_3 = -1$ and $m = 2$ (Eq. 2). If a subunit is added to strand 1, m increases by 1. As in Eqs. 45 and 47,

$$\alpha_1/\beta_1 = \alpha x/\beta; \quad \alpha_1 = \alpha x^{f_1}, \quad \beta_1 = \beta x^{f_1-1}. \quad (56)$$

If a subunit is added to strand 2, m decreases by 1:

$$\alpha_2/\beta_2 = \alpha/\beta x; \quad \alpha_2 = \alpha x^{-f_2}, \quad \beta_2 = \beta x^{1-f_2}. \quad (57)$$

If a subunit is added to strand 3 (to give $m_2 = -2$, $m_3 = 0$), there is no change in m; the rate constants are α and β.

It is not difficult to construct the kinetic diagram for this case, analogous to Fig. 6. However, here the diagram is a two-dimensional array of states associated with the possible values of $m_2 = 0, \pm 1, \ldots$ and of $m_3 = 0, \pm 1, \ldots$. Unfortunately, it does not seem possible to deduce the steady-state state probabilities, analytically, from the diagram. We turn, therefore to the Monte Carlo approach.

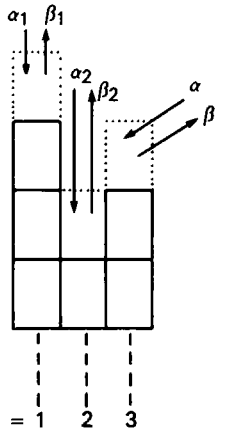

FIGURE 7 Three types of rate constant pairs for case 0:3.

In all of the Monte Carlo calculations in this section (case 0:3) and in Section 5 (cases 1:3 and 2:5), we take all $f_i = 0$ (diffusion controlled attachment; all interaction effects in β). All on rate constants are then α and the off rate constants are calculated as follows, in the course of the computer simulation. In the simulation, we follow the stochastic succession of detailed surface states (characterized by the m_i) passed through by the end of the polymer. In a particular state of the sequence, a subunit might add to any of the strands (with first-order rate constant αc) or a subunit might be lost from any one of the strands. The off rate constant must be calculated for each strand. Let β' be the off constant for an arbitrary strand. To find β', first the value of m is calculated from the m_i (Eq. 2) in the initial state. This is $m(\nu)$ in Eq. 12. With a subunit removed from the arbitrary strand, m is recalculated from the new set of m_i to give $m(\lambda)$. Then $\Delta m \equiv m(\nu) - m(\lambda)$ is related to ΔG_s in Eq. 12 by $\Delta G_s = w_h \Delta m$. Note that Δ is defined in both cases in the direction of adding a subunit. Then Eq. 16 becomes (because $\alpha' = \alpha$)

$$e^{-\Delta G_s/kT} = e^{w_h \Delta m/kT} = x^{\Delta m} = \beta/\beta', \quad \beta' = \beta x^{-\Delta m}. \quad (58)$$

Examples are $\beta_1 = \beta x^{-1}$, $\beta_2 = \beta x$, and $\beta_3 = \beta$ in Eqs. 56 and 57.

For any particular surface state in the stochastic sequence of states, there are (for the 0:3 case) 6 possible transitions (3 on, 3 off), each with a definite first-order rate constant. The reciprocal of the sum of these 6 rate constants gives the mean lifetime of the state, which is used in time-averaging various quantities of interest (e.g., m, m^2, $|m_2|$, etc.) over all states in the sequence. The actual transition selected, that produces the next state in the sequence, is determined by a random number generator; the probability of a given transition (one of 6) is proportional to the corresponding first-order rate constant.

The mean (time averaged) off rate constant is calculated for each strand; these in turn are averaged over all strands (they differ because of fluctuations) to give $\bar{\beta}$. Then $J = \alpha c - \bar{\beta}$. As a check on the program, J is also calculated by

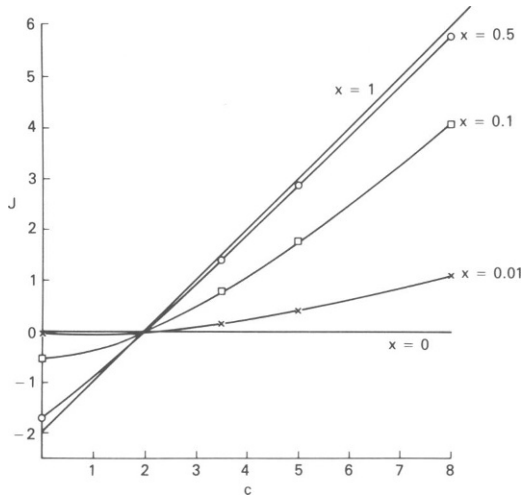

FIGURE 8 $J(c)$ Monte Carlo results at steady state for 0:3 case with $f_1 = f_2 = 0$, $\alpha = 1$, and $\beta = 2$.

the actual counting of individual on and off transitions; this latter J fluctuates more and is therefore less reliable.

The number of transitions used to obtain averages varied from 10,000 to 40,000 (in Section 5, 50,000 for 1:3 and 60,000 for 2:5), depending on the extent of fluctuations in the different cases (values of c and x). Monte Carlo results at $c = c_e$ could be compared with exact equilibrium properties, as a further check on the program.

All steady-state calculations (in this section and Section 5) were made using the reference values $\alpha = 1$ and $\beta = 2$ ($c_e = 2$). Because $\beta = \beta_o x$ (Eq. 55), this means in effect that when x was changed β_o was also adjusted to keep $\beta_o x$ constant. This procedure was adopted to expose surface effects rather than bulk effects.

Fig. 8 gives Monte Carlo $J(c)$ results for the 0:3 case at three different x values. The asymptotic straight lines $\alpha c - \beta$ ($x \to 1$; independent strands) and $J = 0$ ($x \to 0$) are included for reference. $J(c)$ is decidedly nonlinear at $x = 0.1$ and 0.01 because $\bar{\beta}(c)$ is not a constant. This is contrary to conventional belief. Fig. 9 shows $\bar{m}(c)$ in the same examples. These are essentially also $\bar{q}(c)$ curves because $\bar{q} = 2\bar{m}/3$ (Eq. 8). Surface roughness, as measured by $\bar{m}$ or $\bar{q}$, increases with c because on transitions become more dominant and these occur at random on the three strands. As $x \to 0$, $\bar{m} \to 0$ (the surface approaches flatness). Of course J and $\bar{m}$ at $c = c_e = 2$ have equilibrium values (Eq. 27 and Fig. 4).

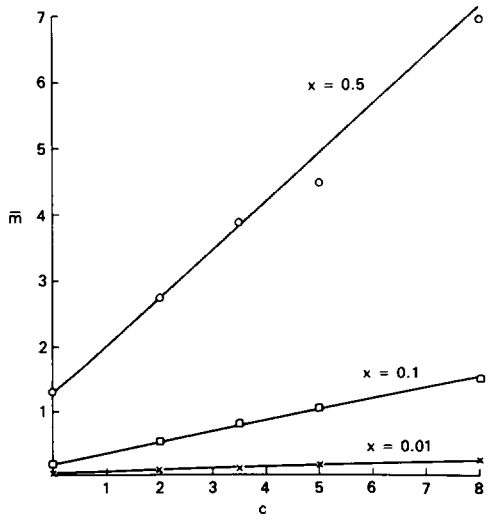

FIGURE 9 Results for $\bar{m}(c)$, corresponding to Fig. 8.

Table IV contains Monte Carlo values of $\sigma_m^2/\bar{m}^2$ and $\sigma_q^2/\bar{q}^2$ (the separate $\bar{m}$, and hence $\bar{q} = 2\bar{m}/3$, values are shown in Fig. 9). The large values in Table IV at $x = 0.01$ and $c = 0$ arise from $\bar{m} = 0.01522$, $\sigma_m^2 = 0.01515$, $\bar{q} = 0.01021$, and $\sigma_q^2 = 0.01021$. The probability distributions in m and q were also calculated but are omitted to save space.

4. EQUILIBRIUM PROPERTIES OF STAGGERED MODELS

We consider in this section a sampling of tubular staggered (helical) models of the type shown in Figs. 1 *a*, 1 *b* and 2. In many cases we merely give the surface partition function Q; $\bar{m}$ and σ_m^2 are easy to derive, if desired, from Eqs. 6 and 7. We give most details about the cases 1:2 (related to actin), 1:3, and 2:5. The fractional stagger in the latter two cases (1/3 and 2/5) is similar to that in a microtubule (5/13 = 0.385).

We begin with the simplest case, 1:2 (Figs. 2 *a*, 3 *a*, and 10 *b*). However, first we digress to point out that the 1:2 model is formally identical to a realistic model for polymerized actin. In Fig. 10 *a*, each subunit in the actin-like structure has two interactions w_h with neighbors. The same is true in the 1:2 case (Fig. 10 *b*) because of the assumed tubular configuration (Fig. 3 *a*). Thus, in bulk polymer,

TABLE IV
MONTE CARLO STEADY-STATE PROPERTIES FOR THE CASE 0:3

x	c	$\sigma_m^2/\bar{m}^2$	$\sigma_q^2/\bar{q}^2$
0.01	0	65.4	97.9
	2	16.9	26.3
	3.5	9.92	14.8
	5	6.21	9.53
	8	3.81	6.02
0.1	0	5.48	8.40
	2	1.74	2.91
	3.5	1.12	1.85
	5	0.977	1.60
	8	0.688	1.25
0.5	0	0.731	1.31
	2	0.560	0.964
	3.5	0.518	0.945
	5	0.464	0.826
	8	0.567	1.05

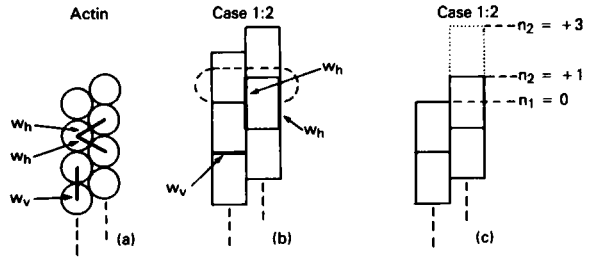

FIGURE 10 (*a*) Model of actin structure, with significance of w_h and w_v. (*b*) Two-stranded staggered case (1:2) with neighbor interactions (w_h and w_v) shown. (*c*) Illustration of n_2 values for case 1:2 ($n_1 = 0$ always).

both structures have an interaction free energy of $w_h + w_v$ per subunit. All of the properties given in this section and in Section 5 (steady state) for the 1:2 case apply as well to the model of actin in Fig. 10 *a*.

As explained in Section 1, it is convenient to use $x^m = y^n$ here, where $n = 2m$ and $x = e^{w_h/kT} = y^2$. As can be seen from Fig. 10 *c*, $n_1 \equiv 0$ and $n_2 = \pm 1, \pm 3, \ldots$. The surface can never be flat. In Eq. 3, $n = |n_2|$. Hence

$$Q = 2(y + y^3 + y^5 + \cdots) = 2y/(1 - y^2) = 2x^{1/2}/(1 - x). \quad (59)$$

Then, from Eqs. 6 and 7,

$$\bar{m} = (1 + x)/2(1 - x), \quad \sigma_m^2 = x/(1 - x)^2. \quad (60)$$

From Eqs. 5 and 59, the probability of a given n is

$$P_n^* = 2y^n/Q \quad (n = 1, 3, 5, \cdots). \quad (61)$$

When $x \to 0$ and $y \to 0$ (i.e., strong attractive interactions, $w_h \to -\infty$), $\bar{m} \to 1/2$, $\sigma_m^2 \to 0$, and $P_1^* \to 1$. That is, the only important surface structures in this limit are $n_2 = \pm 1$ (Fig. 10 *c*). Successive subunits go onto or off of alternate strands of the polymer; the polymer behaves like a single helix (1-start helical growth). It is generally assumed that this is the situation in actin. The determining factor here is the magnitude of w_h compared to kT, not w_h compared to w_v (the value of w_v has no influence on surface structure).

We consider next case 1:3, already illustrated in Figs. 1 *a*, 1 *b*, and 2 *b*. As mentioned at the beginning of Section 1, this system has the same properties as 2:3. We use $x = e^{w_h/kT} = y^3$ and $n = 3m$ (Section 1). Q can be found analytically by summing $x^m = y^n$ over $n_3 = \ldots, -4, -1, 2, 5, \ldots$ for each of $n_2 = \ldots, -5, -2, 1, 4, \ldots$ (with $n_1 = 0$ in all cases). One finds from these series the closed expression

$$Q = 3y^2(1 + y^2)/(1 - y^3)^2. \quad (62)$$

Either by expansion of Eq. 62 or by computer enumeration, we also have

$$Q = \sum_n S(n)y^n = 3(y^2 + 2y^5 + 3y^8 + \cdots + y^4 + 2y^7 + 3y^{10} + \cdots). \quad (63)$$

This provides P_n^* (Eq. 5), the probability of a given n. The leading term in Eq. 63 is $3y^2$, which has $n = 2$. There are 3 structures with $n = 2$. Thus, the smallest possible value of m is 2/3 (i.e., $m = n/3$). The structures in both Figs. 1 *a* and 2 *b* have $m = 2/3$; the surface cannot be flat.

From Eqs. 6 and 7,

$$\bar{m} = \frac{2(1 + 2y^2 + 2y^3 + y^5)}{3(1 - y^3)(1 + y^2)} \quad (64)$$

$$\sigma_m^2 = \frac{2y^2(2 + 9y + 14y^3 + 9y^5 + 2y^6)}{9(1 - y^3)^2(1 + y^2)^2}. \quad (65)$$

The curve $\bar{m}$ as a function of $-w_h/kT$ is included in Fig. 4.

It will be recalled (Eq. 8) that r represents any one of the terms in the sum in Eq. 3, for example, $|n_2|$. This is the height difference between nearest neighbor strands measured in thirds. The mean value of r is related to $\bar{m}$ by $\bar{r} = 2\bar{m}$ (Eq. 8). Hence Fig. 4 gives essentially $\bar{r}$ as a function of $-w_h/kT$. The probability distribution in r, p_r^*, follows from $U(r, n)$ (Eq. 11), which can be obtained by computer. The $U(r, n)$ table in this case (not shown) is very simple (almost all entries are 0 or 6). From Eq. 11, we obtain

$$p_1^* = 2y^2/Q(1 - y^3) \quad (66)$$

$$p_r^* = \frac{[(r + 1)/3]y^r(1 - y^3) + 2y^{r+2}}{Q(1 - y^3)} \cdot (r = 2, 5, 8, \cdots) \quad (67)$$

$$= \frac{[(r - 1)/3]y^r(1 - y^3) + 2y^{r+1}}{Q(1 - y^3)} \cdot (r = 4, 7, 10, \cdots) \quad (68)$$

with Q given by Eq. 62.

In the limit $x \to 0$ and $y \to 0$ (strong horizontal interactions),

$$Q \to 3y^2, \quad \bar{m} \to 2/3, \quad \bar{n} \to 2, \quad \bar{r} \to 4/3, \quad P_2^* \to 1, \quad p_1^* \to 2/3, \quad p_2^* \to 1/3. \quad (69)$$

This set of limits corresponds physically to the use of only three surface structures: $n_i = 0, 1, 2$; $n_i = 0, 1, -1$; and $n_i = 0, -2, -1$. The first two structures are those in Figs. 2 *b* and 1 *a*, respectively. The polymer gains or loses subunits only via a single right-handed 1-start helix.

In the remaining cases considered in this section, Q was obtained from Eq. 4 after computer tabulation of $S(n)$. Several series had to be summed in each case, some of them rather complicated. Details are omitted. Considerable computer time is needed for $s \geq 8$. The cases included here are 1:4, 2:4, 1:5, 2:5, 1:6, 2:6, 3:6, and 4:8. These cases, with 1:2 and 1:3 above, comprise a complete set of staggered tubes for $s = 2$ through 6.

For cases of type 1:s, we already have 1:2 (Eq. 59) and

1:3 (Eq. 62). In addition,

$$Q = \frac{4y^3(1 + 3y^3 + y^6)}{(1 - y^4)^3} \quad (1{:}4,\ x = y^4) \tag{70}$$

$$Q = \frac{5y^4(1 + 6y^4 + 6y^8 + y^{12})}{(1 - y^5)^4} \quad (1{:}5,\ x = y^5) \tag{71}$$

$$Q = \frac{6y^5(1 + 10y^5 + 20y^{10} + 10y^{15} + y^{20})}{(1 - y^6)^5} \quad (1{:}6,\ x = y^6). \tag{72}$$

The expressions for $\bar{m}$ and σ_m^2 are easy to derive (Eqs. 6 and 7). The coefficients in the Q sums are the same as in Eqs. 38 and 39.

In the limit $x \to 0$, $y \to 0$ (strong horizontal interactions), $Q \to sy^{s-1}$ for the general case 1:s. The surface has regular steps, as shown in Fig. 2 *b* (for 1:3). The lowest step can be at any strand; hence the degeneracy factor s in Q. With regular steps, it is easy to see that $n = s - 1$. In other words, in this limit for any s, the polymer gains and loses subunits only via a single right-handed 1-start helix.

As one would expect, it is possible, using a modification of Eq. 38 in Q for arbitrary s, to show that Eq. 41 holds for $\bar{m}$ here in the limit $s \to \infty$.

Another connected series of cases is 1:2, 2:4, 3:6, and 4:8. The Q for 1:2 is given in Eq. 59. For the other cases,

$$Q = \frac{2y^4(3 + 4y^2 + 3y^4)}{(1 - y^4)^3} \quad (2{:}4,\ x = y^4) \tag{73}$$

$$Q = \frac{4y^9(5 + 15y^3 + 23y^6 + 15y^9 + 5y^{12})}{(1 - y^6)^5} \quad (3{:}6,\ x = y^6) \tag{74}$$

$$Q = \frac{2y^{16}(35 + 168y^4 + 399y^8 + 512y^{12} + 399y^{16} + 168y^{20} + 35y^{24})}{(1 - y^8)^7} \quad (4{:}8,\ x = y^8). \tag{75}$$

The remaining two examples studied are 2:5 and 2:6. In the latter case,

$$Q = \frac{3y^8(5 + 2y^2 + 20y^4 + 15y^6 + 15y^8 + 20y^{10} + 2y^{12} + 5y^{14})}{(1 - y^6)^5} \quad (2{:}6,\ x = y^6). \tag{76}$$

In the former case, which will also be considered at steady state in Section 5,

$$Q = \frac{5y^6(2 + y^2 + 4y^3 + 4y^5 + y^6 + 2y^8)}{(1 - y^5)^4} \quad (2{:}5,\ x = y^5). \tag{77}$$

From Eq. 6 (for 2:5),

$$\bar{m} = \frac{4(3 + 2y^2 + 9y^3 + 18y^5 + 3y^6 + 3y^7 + 18y^8 + 9y^{10} + 2y^{11} + 3y^{13})}{5(1 - y^5)(2 + y^2 + 4y^3 + 4y^5 + y^6 + 2y^8)}. \tag{78}$$

In the limit $x \to 0$, $y \to 0$, we have $\bar{m} \to 6/5$. Fig. 4 includes $\bar{m}$ as a function of $-w_h/kT$.

From a rather complicated $U(r, n)$ table (in the 2:5 case), obtained by computer, we find for the p_r^* (Eq. 11),

$$p_2^* = \frac{2y^6(3 + 2y^2 + 2y^3 + 3y^5)}{Q(1 - x)^3} \tag{79}$$

$$p_r^* = \frac{2}{Q}\left\{\frac{k(k+1)(k+2)y^r}{12} + \frac{2y^{r+9}}{(1-x)^3} + \frac{3y^{r+6}[2 + k(1-x)]}{(1-x)^3} + \frac{y^6[(k+1)(k+2)x^k(1-x)^2 + 2x^{k+1}\langle k + 2 - (k+1)x\rangle]}{(1-x)^3}\right\}$$

$$k = (r - 3)/5, \quad r = 3, 8, 13, \cdots \tag{80}$$

$$p_r^* = \frac{2}{Q}\left\{\frac{j(j+1)(j+2)y^r}{12} + \frac{2y^{r+6}}{(1-x)^3} + \frac{3y^{r+4}[2 + j(1-x)]}{(1-x)^3} + \frac{y^9[(j+1)(j+2)x^j(1-x)^2 + 2x^{j+1}\langle j + 2 - (j+1)x\rangle]}{(1-x)^3}\right\}$$

$$j = (r - 7)/5, \quad r = 7, 12, 17, \cdots \tag{81}$$

When $x \to 0$ and $y \to 0$, $Q \to 10y^6$. There are 10 different surface structures with the five r values 2, 2, 2, 3, 3. These r values, on summing, give $n = 12/2 = 6$. Also, $\bar{r} = 12/5$, $\bar{m} = \bar{r}/2 = 6/5$, $p_2^* = 3/5$, and $p_3^* = 2/5$. Two of the 10 surface structures are shown in Fig. 11 (any one of the five strands can have the lowest position).

5. STAGGERED MODELS AT STEADY STATE

We consider three cases, 1:2, 1:3, and 2:5. The first can be handled analytically. The other two require Monte Carlo

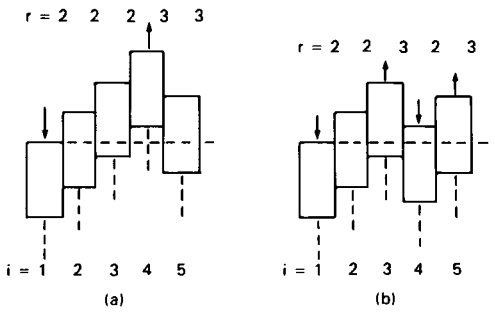

FIGURE 11 The two types of most stable surface structure for the case 2:5. In (*a*), $r = 2, 2, 2, 3, 3$; in (*b*) $r = 2, 2, 3, 2, 3$. In both examples $i = 1$ is the lowest strand but any of the others can be. Arrows show subunit additions or departures that leave the surface free energy unchanged.

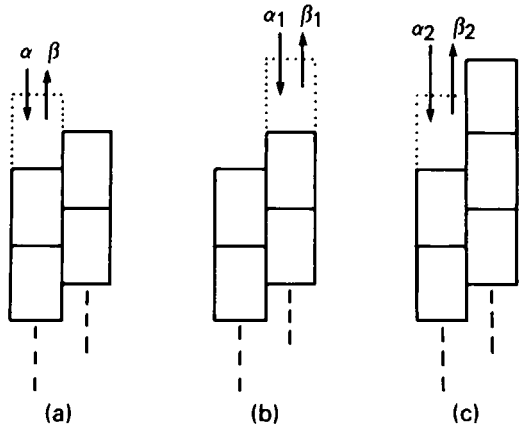

FIGURE 12 Three types of rate constant pairs for case 1:2.

calculations. As already mentioned, 1:2 is equivalent to polymeric actin, whereas 1:3 and 2:5 resemble microtubules (5:13) in the fractional extent of stagger (1/3, 2/5, 5/13).

The algebra in the 1:2 case is similar to that for 0:2 (Section 3). Fig. 12 shows the three sets of rate constants that arise for 1:2. In Fig. 12 *a*, there is no change in surface free energy. Hence the rate constants are the reference constants α and β. In Fig. 12 *b*, $\Delta n = 2$ and $\Delta m = 1$ (on addition of a subunit). In Fig. 12 *c*, $\Delta n = -2$ and $\Delta m = -1$. Therefore Eqs. 45–47 all apply to the present model. The kinetic diagram in terms of n values is shown in Fig. 13. The rate constants are unchanged between pairs of successive states in the linear diagram. Each state (n value) is doubly degenerate (exchange strands). The rate constants α and β apply between the two substates of $n = 1$ (Fig. 12 *a*), but they do not appear in Fig. 13 (however, see $\bar{\alpha}$ and $\bar{\beta}$ below). Because the diagram is linear, there is a "detailed balance" solution at steady state (as for Fig. 6). The successive states $n = 1, 3, 5, \ldots$ have relative probabilities $1, z, z^2 \ldots$, where z is the same as in Eq. 49. Hence the normalized probabilities are

$$P_n^* = z^{(n-1)/2}(1 - z) \quad (n = 1, 3, 5, \cdots). \tag{82}$$

At equilibrium ($\alpha c = \beta$), $z = x = y^2$, thus recovering Eq. 61. From Eq. 82, using $n = 2m$, we find

$$\bar{m} = (1 + z)/2(1 - z), \quad \sigma_m^2 = z/(1 - z)^2. \tag{83}$$

These are generalizations of Eqs. 60.

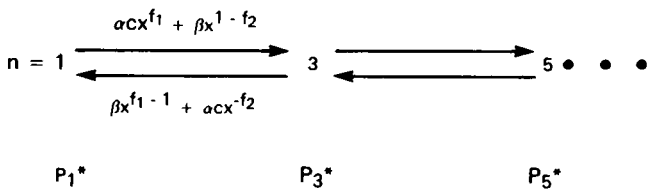

FIGURE 13 Kinetic diagram for case 1:2 in terms of n values of surface structures. Rate constants for $3 \rightleftharpoons 5$, etc., are the same as those for $1 \rightleftharpoons 3$.

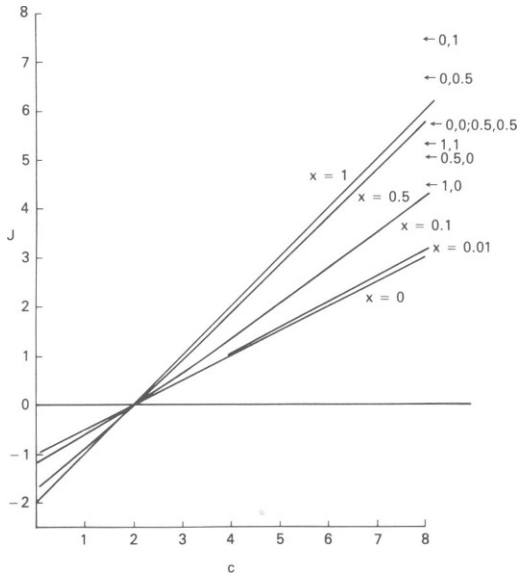

FIGURE 14 Curves are analytical results for $J(c)$ in case 1:2 with $f_1 = f_2 = 0$, $\alpha = 1$, and $\beta = 2$. Short arrows at $c = 8$ show values of J at $c = 8$ for $x = 0.5$ but with different pairs f_1, f_2.

The total subunit on rate for both strands is $\alpha c + \alpha c x^{f_1}$ when $n = 1$ and is $\alpha c x^{f_1} + \alpha c x^{-f_2}$ for all other values of n. The corresponding off rates are $\beta + \beta x^{1-f_2}$ for $n = 1$ and $\beta x^{f_1-1} + \beta x^{1-f_2}$ otherwise. Using $P_1^* = 1 - z$ and $1 - P_1^* = z$, we find for the mean rate constants per strand

$$\bar{\alpha}(c) = (\alpha/2)[(1 - z)(1 + x^{f_1}) + z(x^{f_1} + x^{-f_2})] \tag{84}$$

$$\bar{\beta}(c) = (\beta/2)[(1 - z)(1 + x^{1-f_2}) + z(x^{f_1-1} + x^{1-f_2})]. \tag{85}$$

These then give $J = \bar{\alpha}c - \bar{\beta}$, the mean subunit flux per

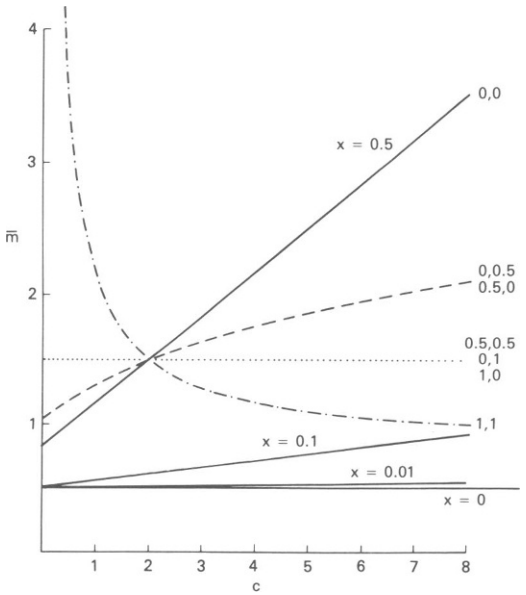

FIGURE 15 Results for $\bar{m}(c)$, corresponding to Fig. 14. The nonsolid curves are for $x = 0.5$ and different pairs f_1, f_2.

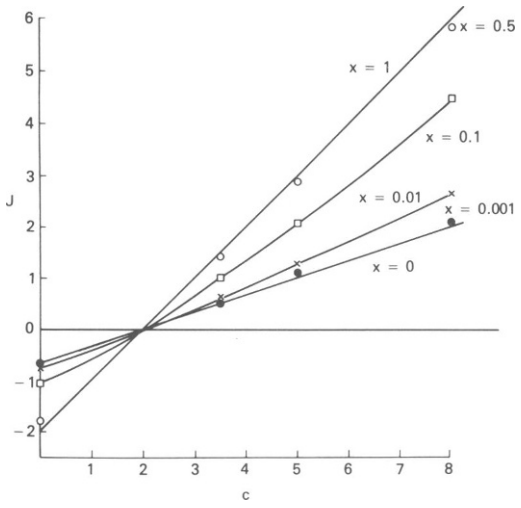

FIGURE 16 $J(c)$ Monte Carlo results at steady state for 1:3 case with $f_1 = f_2 = 0$, $\alpha = 1$, and $\beta = 2$.

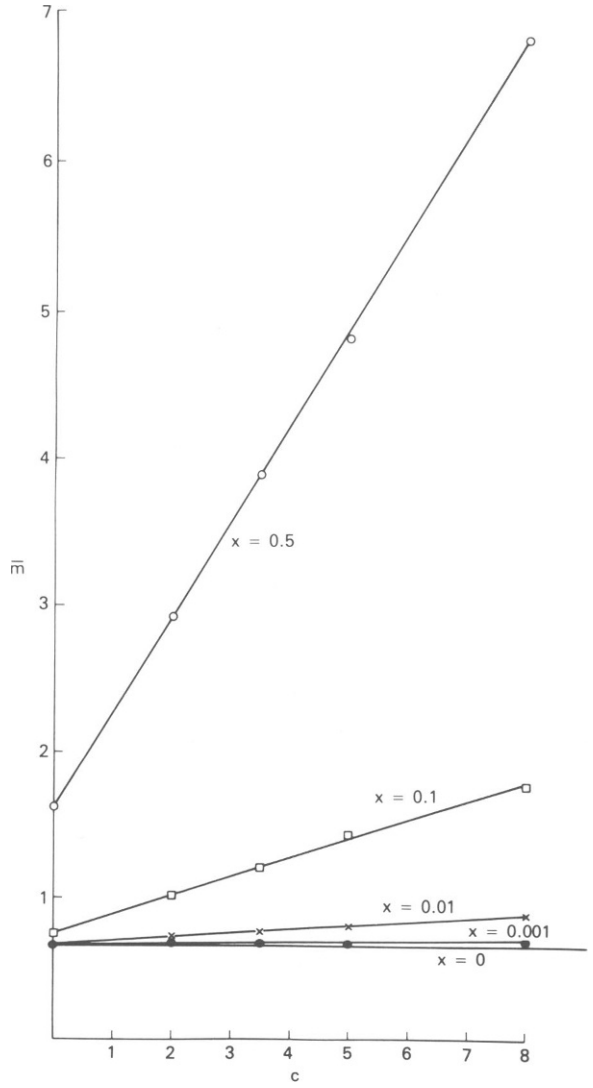

FIGURE 17 Results for $\bar{m}(c)$ corresponding to Fig. 16.

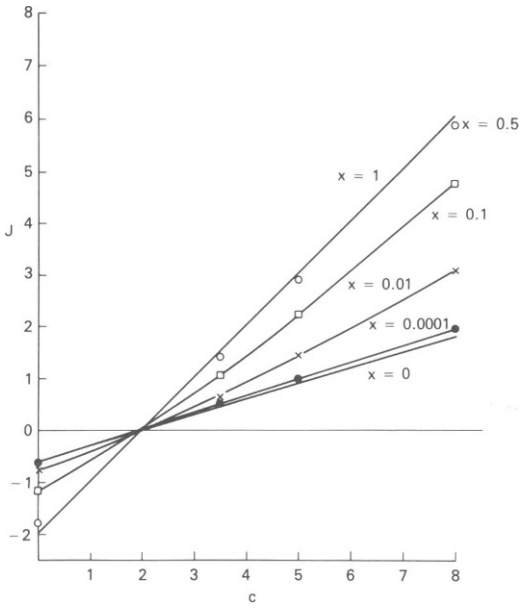

FIGURE 18 $J(c)$ Monte Carlo results at steady state for 2:5 case with $f_1 = f_2 = 0$, $\alpha = 1$, and $\beta = 2$.

strand. At equilibrium ($z = x$),

$$\bar{\alpha} = (\alpha/2)(1 + x^{f_1} - x + x^{1-f_2}) \tag{86}$$

$$\bar{\beta} = (\beta/2)(1 + x^{f_1} - x + x^{1-f_2}) \tag{87}$$

Thus $\bar{\alpha}/\bar{\beta} = \alpha/\beta$ (Eq. 20).

When $x \to 0$ and f_1 and f_2 are between 0 and 1, $z \to 0$ and $\bar{\alpha} \to \alpha/2$, $\bar{\beta} \to \beta/2$. The polymer behaves as if it has

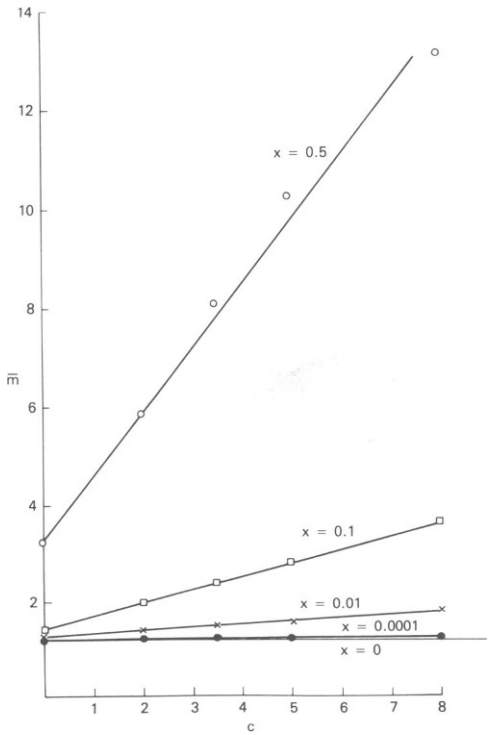

FIGURE 19 Results for $\bar{m}(c)$ corresponding to Fig. 18.

TABLE V
MONTE CARLO STEADY-STATE PROPERTIES FOR THE CASE 1:3

x	c	$\sigma_m^2/\overline{m}^2$	$\sigma_q^2/\overline{q}^2$
0.001	0	0.000342	0.125
	2	0.0138	0.142
	3.5	0.0251	0.157
	5	0.0368	0.169
	8	0.0681	0.222
0.01	0	0.00620	0.133
	2	0.0752	0.228
	3.5	0.125	0.296
	5	0.165	0.347
	8	0.258	0.501
0.1	0	0.111	0.278
	2	0.307	0.564
	3.5	0.357	0.632
	5	0.407	0.708
	8	0.403	0.738
0.5	0	0.490	0.860
	2	0.445	0.796
	3.5	0.489	0.866
	5	0.501	0.871
	8	0.482	0.895

TABLE VI
MONTE CARLO STEADY-STATE PROPERTIES FOR THE CASE 2:5

x	c	$\sigma_m^2/\overline{m}^2$	$\sigma_q^2/\overline{q}^2$
0.001	0	0.000133	0.0422
	2	0.00338	0.0585
	3.5	0.00664	0.0719
	5	0.00905	0.0874
	8	0.0192	0.109
0.01	0	0.00963	0.0755
	2	0.0541	0.229
	3.5	0.0792	0.327
	5	0.111	0.413
	8	0.157	0.537
0.1	0	0.0774	0.300
	2	0.156	0.546
	3.5	0.190	0.699
	5	0.225	0.758
	8	0.232	0.808
0.5	0	0.216	0.759
	2	0.246	0.801
	3.5	0.235	0.785
	5	0.247	0.795
	8	0.252	0.997

only one strand ($n_2 = \pm 1$); subunits alternate strands in their arrivals and departures, using the reference rate constants α and β (Fig. 12 *a*).

In the important special case $f_1 = f_2 = 0$, z is given in Eq. 54 and

$$\bar{\alpha} = \alpha, \quad \bar{\beta} = (\beta/2)(1 + x - z + zx^{-1}). \tag{88}$$

To illustrate some of the above results, we plot $J(c)$ in Fig. 14 and $\overline{m}(c)$ in Fig. 15 for $\alpha = 1, \beta = 2, f_1 = f_2 = 0$, and $x = 0.5, 0.1$, and 0.01. The $J(c)$ curve in Fig. 14 for $x = 0.1$ is noticeably nonlinear. The $x = 0.01$ curve is close to the asymptotic line discussed above ($x \to 0$), $J = (\alpha c - \beta)/2$. Also, the $x = 0.5$ curve is not far from $J = \alpha c - \beta$ (for $x \to 1$; independent strands).

The behavior of $\overline{m}(c)$ in Fig. 15 is similar to that already seen in Fig. 9 (0:3) except that $\overline{m} = 1/2$ is the lower limit (the surface cannot be flat). The $\overline{m}(c)$ curves are linear in c (Eqs. 54 and 83). The $\overline{m}(c)$ curves in the other examples in this paper (Figs. 9, 17, and 19), all for $f_1 = f_2 = 0$, are also at least approximately linear. In the 0:2 case (Eqs. 50 and 54), $\overline{m}(c)$ is also approximately linear, but it is not exactly linear.

Although most choices are very unrealistic, the effect of varying f_1 and f_2 is also included in Figs. 14 and 15 for the case $x = 0.5$. In Fig. 14, we merely show (short arrows) the value of J at $c = 8$ for $x = 0.5$ and various pairs f_1, f_2. Of course all curves (not shown) pass through $J = 0$, $c = 2$. In Fig. 15, the complete $\overline{m}(c)$ curves are given for $x = 0.5$ and the same set of f_1, f_2 choices. In the 1,1 case, surface free energy effects are confined entirely to the on rate constants; the off rate constant is always β (see Eqs. 47). Hence, when c is small and random off transitions dominate, fluctuations in the strand that loses the subunit can lead to large values of $\overline{m}$. The equilibrium value of $\overline{m}$ (i.e., at $c = 2$) is not influenced by the kinetic parameters f_1, f_2.

Finally, we give Monte Carlo results for 1:3 and 2:5, taking all $f_i = 0$, $\alpha = 1$, and $\beta = 2$. The discussion of the Monte Carlo approach before and after Eq. 58 applies here as well. Figs. 16 and 17 show $J(c)$ and $\overline{m}(c)$, respectively, for 1:3. The $J(c)$ curve for $x = 0.1$ is very nonlinear. The asymptotic $J(c)$ lines are $\alpha c - \beta$ (for $x \to 1$) and $(\alpha c - \beta)/3$ (for $x \to 0$). In the latter limit, growth is via a single right-handed helix (Eq. 69).

Figs. 18 and 19 give $J(c)$ and $\overline{m}(c)$ for 2:5. Distinctly nonlinear $J(c)$ curves are found for $x = 0.1$ and 0.01. The limiting $J(c)$ line for $x \to 0$ is not $(2/5)(\alpha c - \beta)$ as one might expect, but $(3/10)(\alpha c - \beta)$. The reason for this is the following. When $x \to 0$, only 10 surface structures are used ($Q \to 10y^6$ in Eq. 77), all with minimal surface free energy ($n = 6$). Five are of the type in Fig. 11 *a* and 5 of the type in Fig. 11 *b*. In Fig. 11 *b*, there are 2 addition and 2 departure sites that leave the surface structure within the class of 10 (i.e., still with $n = 6$). However, in Fig. 11 *a*, there is only one such site of each type. Hence 2-helix growth cannot be maintained at the nominal rate $(2/5)(\alpha c - \beta)$; 2/5 and 1/5 are averaged to give the factor 3/10 above. A related problem has been discussed for microtubules (1, 5).

Tables V and VI give Monte Carlo values of $\sigma_m^2/\overline{m}^2$ and $\sigma_q^2/\overline{q}^2$ (as in Table IV) for 1:3 and 2:5, respectively. The separate $\overline{m}$ values (also, $\overline{q} = 2\overline{m}/s$) are in Figs. 17 and 19.

These tables differ qualitatively from Table IV at small x because $\overline{m} \to 0$ and $\overline{q} \to 0$ as $x \to 0$ in the Table IV case (0:3) but, in Tables V and VI, $\overline{m}$ and $\overline{q}$ are always finite. Note that because $\overline{r} = s\overline{q}$ and $\sigma_r^2 = s^2\sigma_q^2$, $\sigma_q^2/\overline{q}^2 = \sigma_r^2/\overline{r}^2$.

CONCLUSION

Consideration of fluctuating microscopic surface structures and microscopic rate constants in a class of multistranded "equilibrium" polymers shows that the usual assumption of a linear $J(c)$ curve is not justified except in special cases.

Received for publication 1 July 1985 and in final form 12 November 1985.

REFERENCES

1. Hill, T. L., and M. W. Kirschner. 1982. Bioenergetics and kinetics of microtubule and actin filament assembly-disassembly. *Inter. Rev. Cytol.* 78:1–125.
2. Hill, T. L., and M. -F. Carlier. 1983. Steady-state theory of the interference of GTP hydrolysis in the mechanism of microtubule assembly. *Proc. Natl. Acad. Sci. USA* 80:7234–7238.
3. Hill, T. L. 1985. Cooperativity Theory in Biochemistry. Springer Verlag, New York.
4. Hill, T. L. 1985. Statistical Thermodynamics. Dover Publications, New York.
5. Chen, Y., and T. L. Hill. 1985. Monte Carlo study of the GTP cap in a five-start helix model of a microtubule. *Proc. Natl. Acad. Sci. USA.* 82:1131–1135.